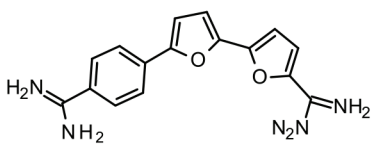
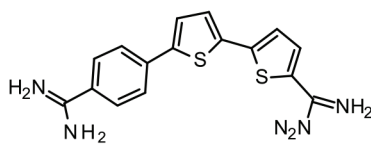


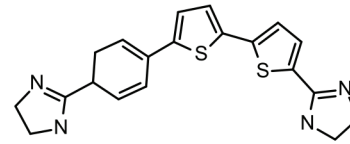
## SUPPLEMENTARY SCHEMES, FIGURES AND TABLES



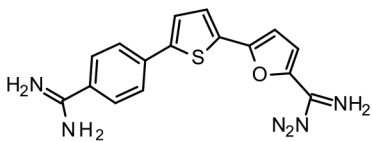
HAD1



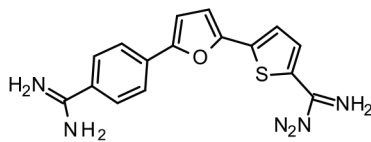
HAD2



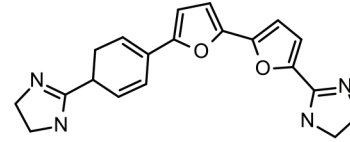
HAD3



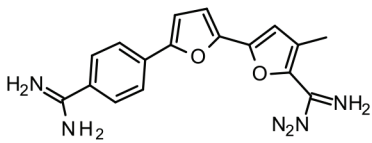
HAD4



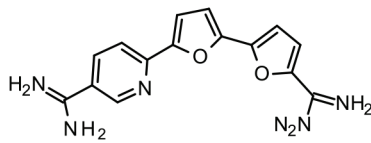
HAD5



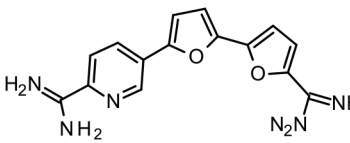
HAD6



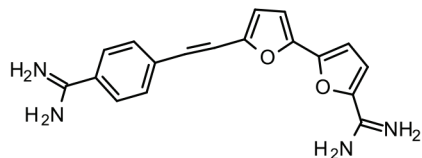
HAD7



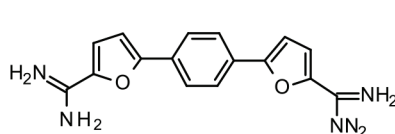
HAD8



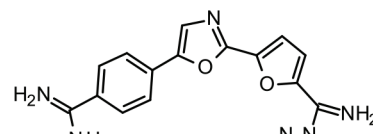
HAD9



HAD10

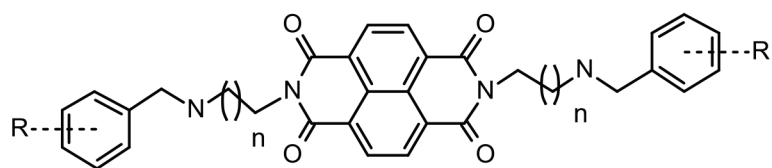


HAD11



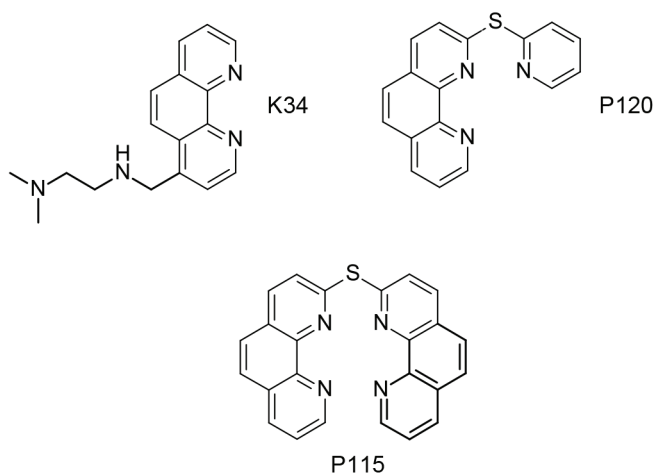
HAD12

Supplementary Scheme S1: Chemical structures of tested HAD derivatives.

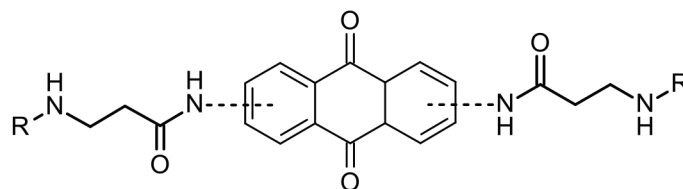


Compound	n	R
NDI1	2	2-OCH <sub>3</sub>
NDI2	1	2-OCH <sub>3</sub>
NDI3	2	2,3,4-OCH <sub>3</sub>
NDI4	2	3,4,5-OCH <sub>3</sub>
NDI5	2	H

Supplementary Scheme S2: Chemical structures of tested NDI derivatives.

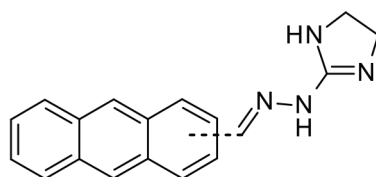


Supplementary Scheme S3: Chemical structures of tested Phen derivatives.



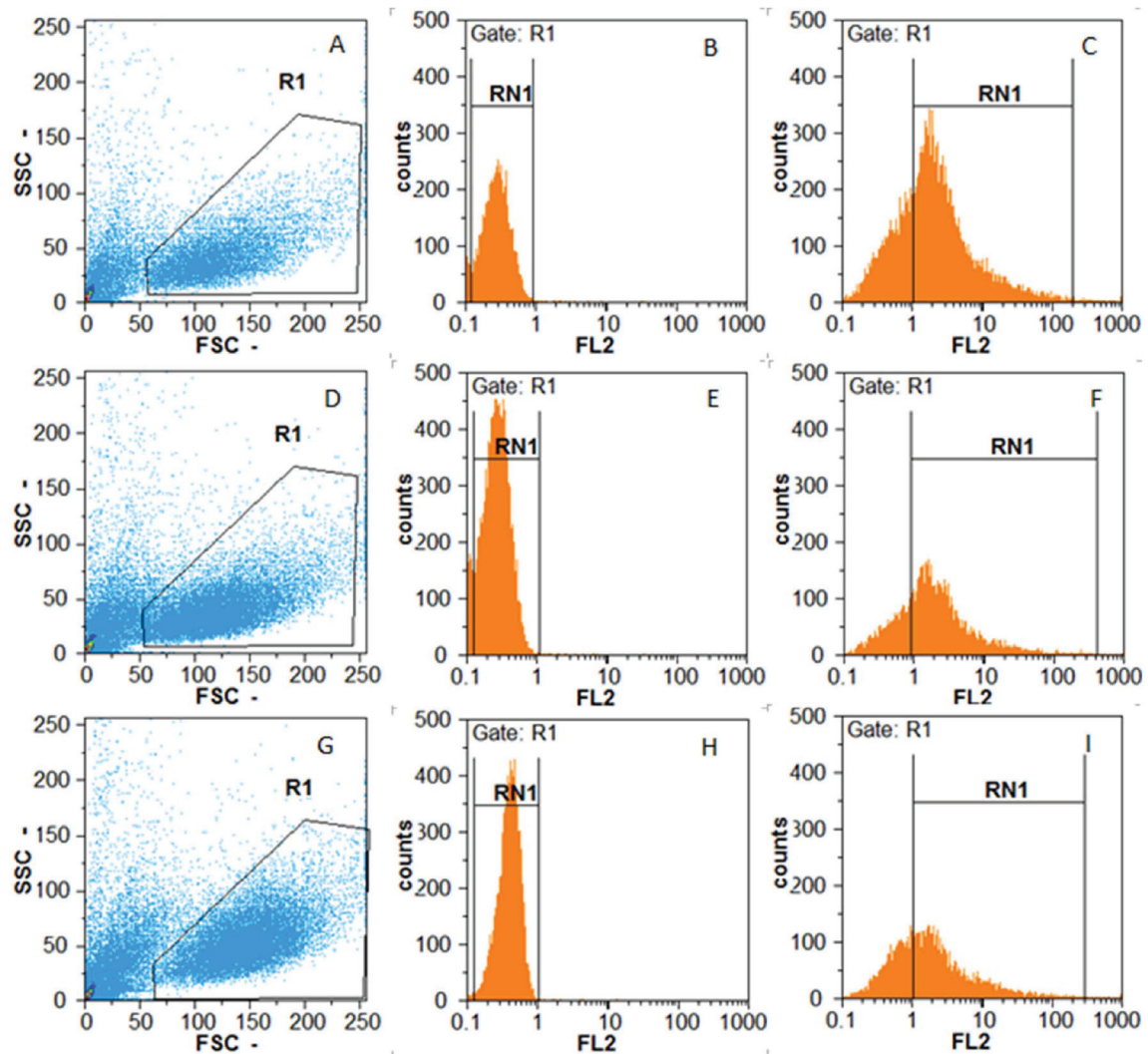
Compound	R	Position
AQ1	Lys	1,5
AQ2	Lys	1,8
AQ3	Lys	2,6
AQ4	Lys	2,7
AQ5	Phe-Lys	1,5
AQ6	Phe-Lys	1,8
AQ7	Phe-Lys	2,6
AQ8	Phe-Lys	2,7

Supplementary Scheme S4: Chemical structures of tested AQ derivatives.

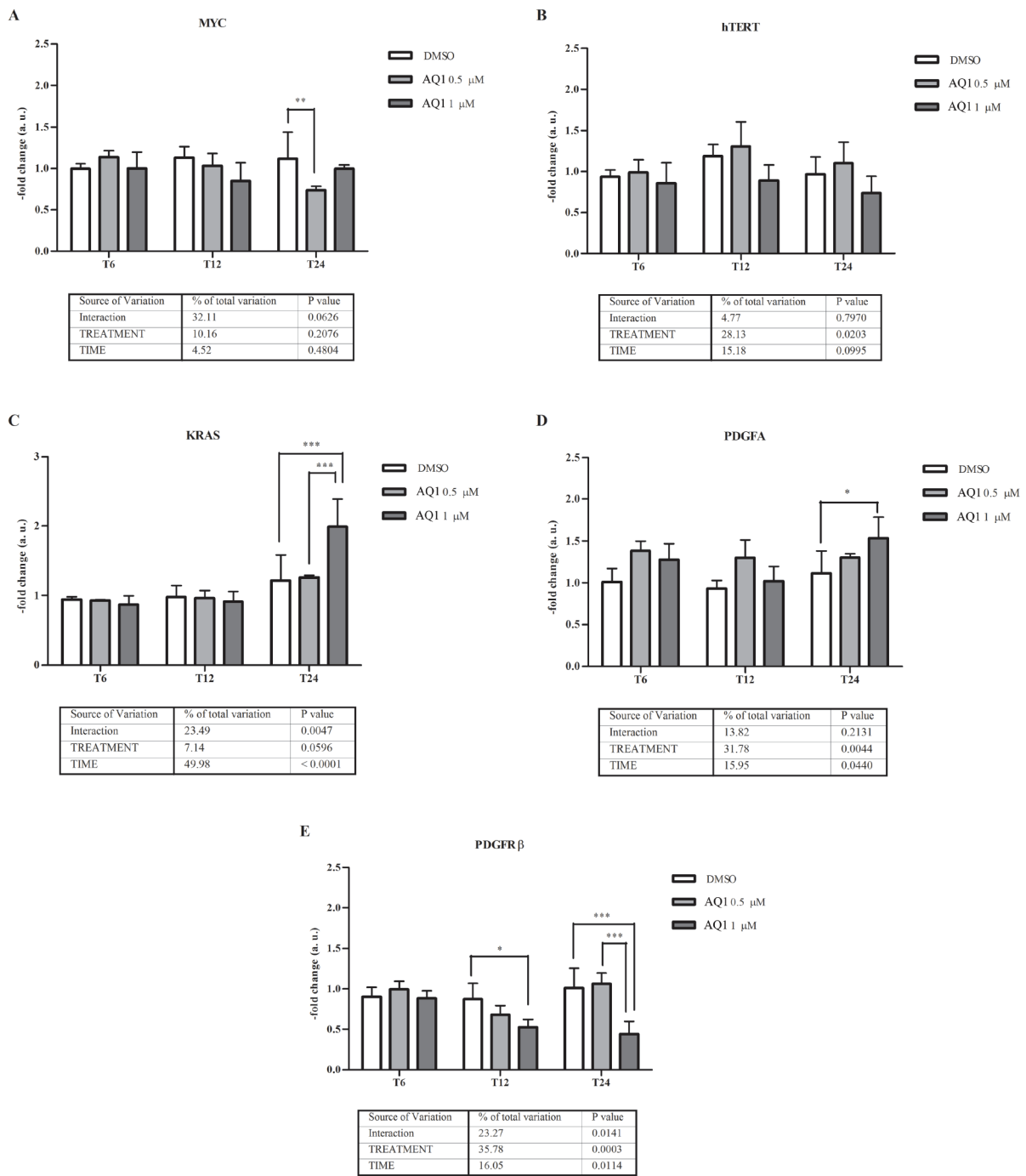


Compound	Position
AN1	1
AN2	2
AN3	9
AN4	9,10
AN5	1,5
AN6	1,8
AN7	2,6
AN8	2,7

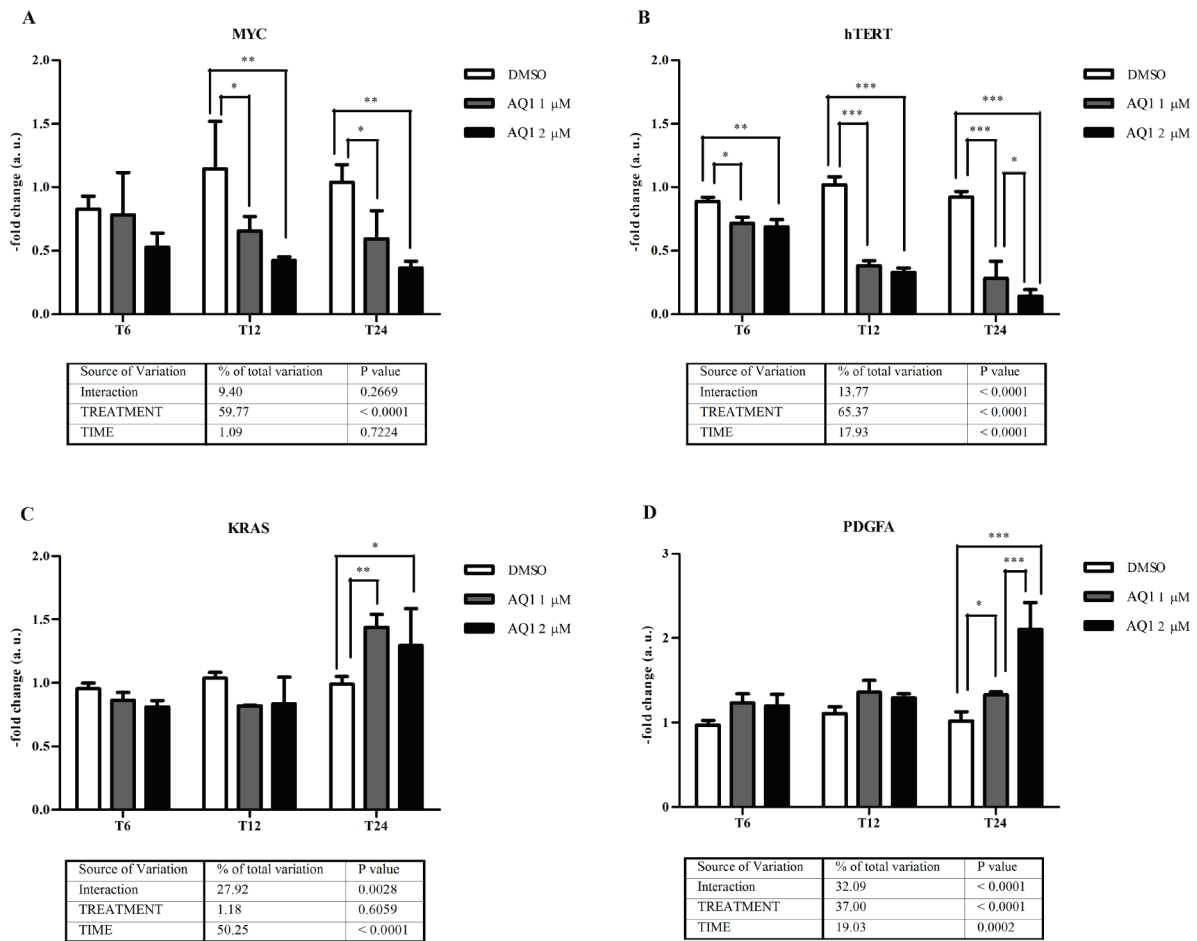
Supplementary Scheme S5: Chemical structures of tested AN derivatives.



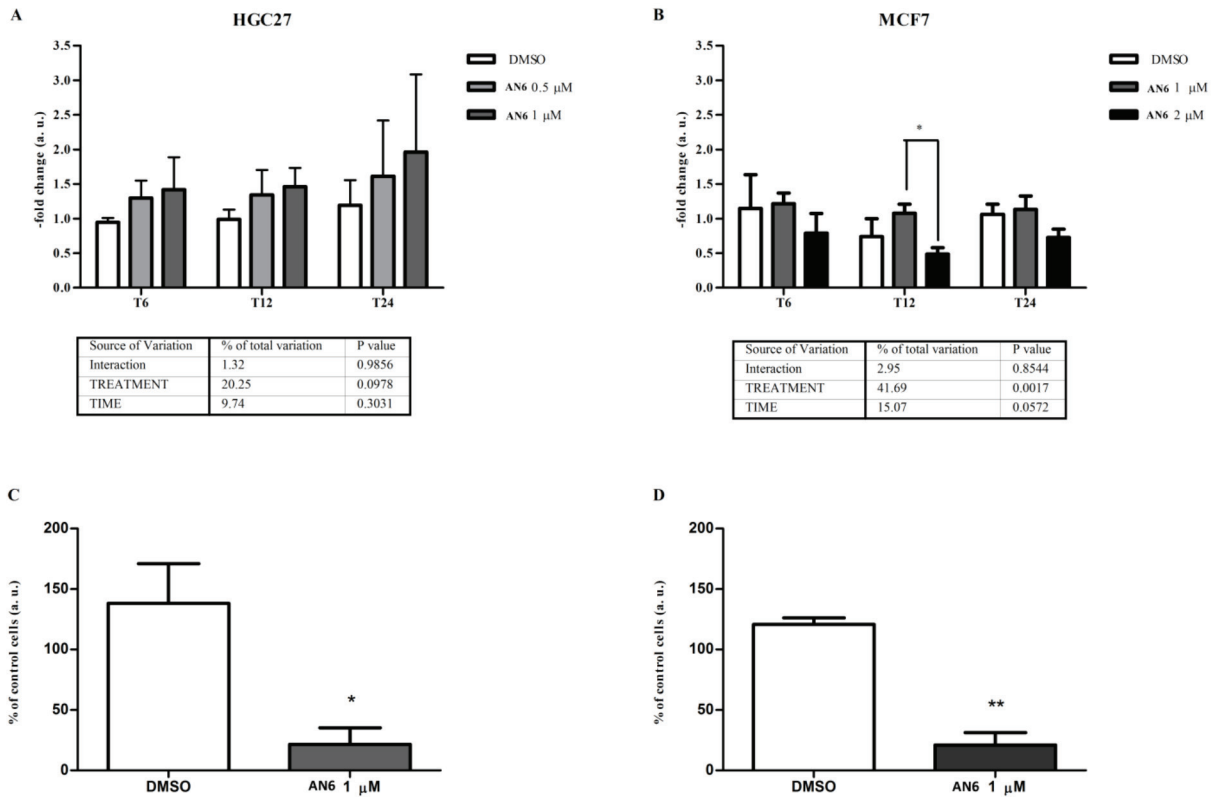
**Supplementary Figure S1: Evaluation of CD117 expression in HCG27 cells after 48h of incubation.** Control sample: **A.** morphological scatter (forward scatter, FSC; side scatter, SSC); **B.** isotype control, histogram; **C.** CD117 expression, histogram. HCG27 cells incubated with DMSO **D.** morphological scatter (forward scatter, FSC; side scatter, SSC); **E.** isotype control, histogram; **F.** CD117 expression, histogram. HCG27 cells incubated with AQ1 1  $\mu$ M: **G.** morphological scatter (forward scatter, FSC; side scatter, SSC); **H.** isotype control, histogram **I.** CD117 expression, histogram.



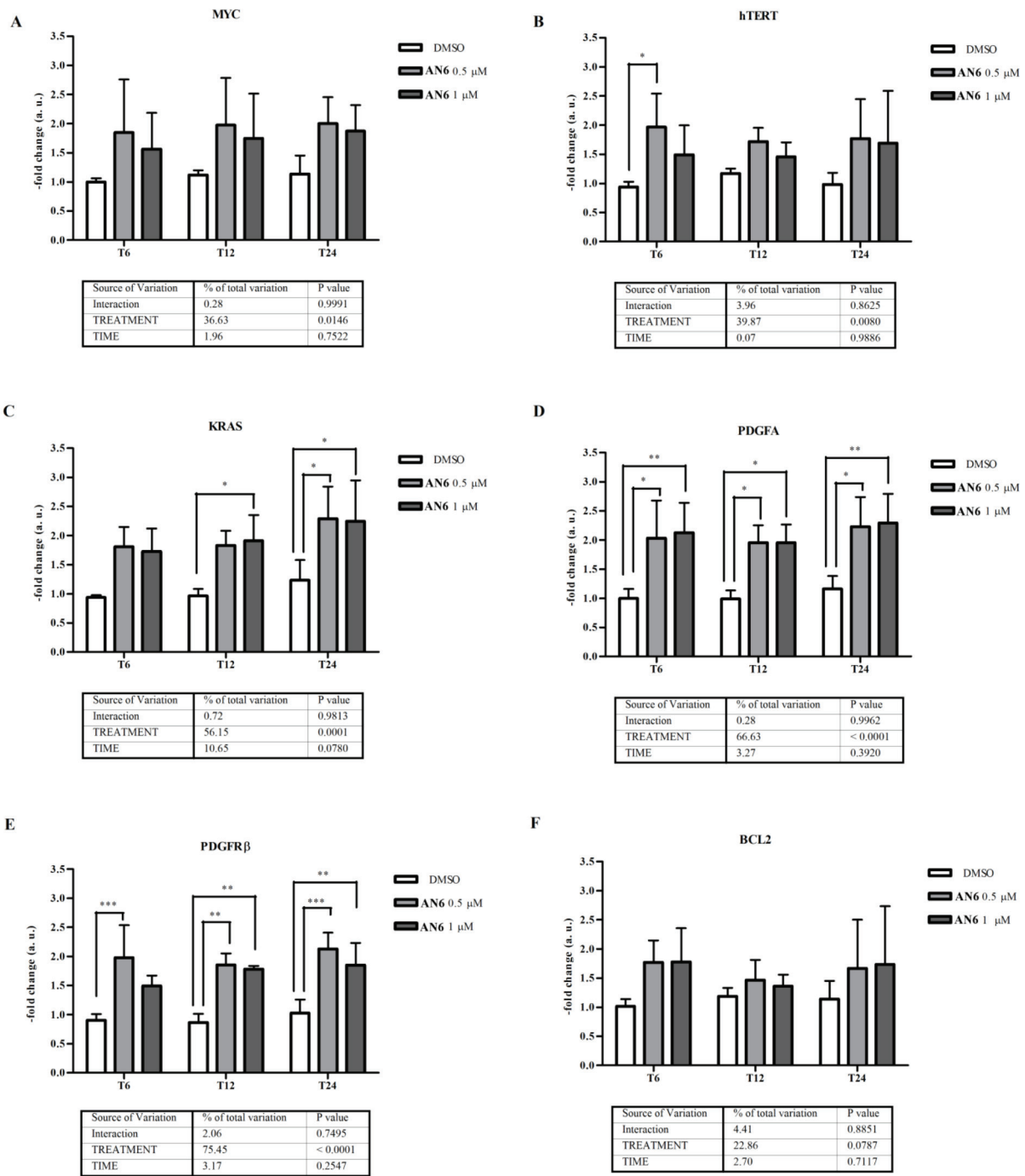
**Supplementary Figure S2: Effect of AQ1 on mRNA of other oncogenes possessing G4 structures in the HGC27 cell line.** A. *MYC*, B. *hTERT*, C. *KRAS*, D. *PDGFA* and E. *PDGFRβ* mRNA levels were measured using qPCR assays, and data (arithmetic means ± S.D.) are expressed as n-fold change (arbitrary units, a.u.) normalized to the RQ of control cells at each time (T<sub>6</sub>, T<sub>12</sub>, T<sub>24</sub>), to whom an arbitrary value of 1 was assigned. Two-way ANOVA and Bonferroni post-test were used to identify statistical differences between doses and time of treatment. \*,\*\*,\*\*\*:  $P < 0.05$ ;  $P < 0.01$ ;  $P < 0.001$ .



**Supplementary Figure S3: Effect of AQ1 on mRNA of oncogenes possessing G4 structures in MCF7 cell line.** A. *MYC*, B. *hTERT*, C. *KRAS* and D. *PDGFA* mRNA levels were measured using qPCR assays, and data (arithmetic means  $\pm$  S.D.) are expressed as n-fold change (arbitrary units, a.u.) normalized to the RQ of control cells at each time ( $T_6$ ,  $T_{12}$ ,  $T_{24}$ ), to whom an arbitrary value of 1 was assigned. Two-way ANOVA and Bonferroni post-test were used to identify statistical differences between doses and time of treatment. \*, \*\*, \*\*\*:  $p < 0.05$ ;  $p < 0.01$ ;  $p < 0.001$ .

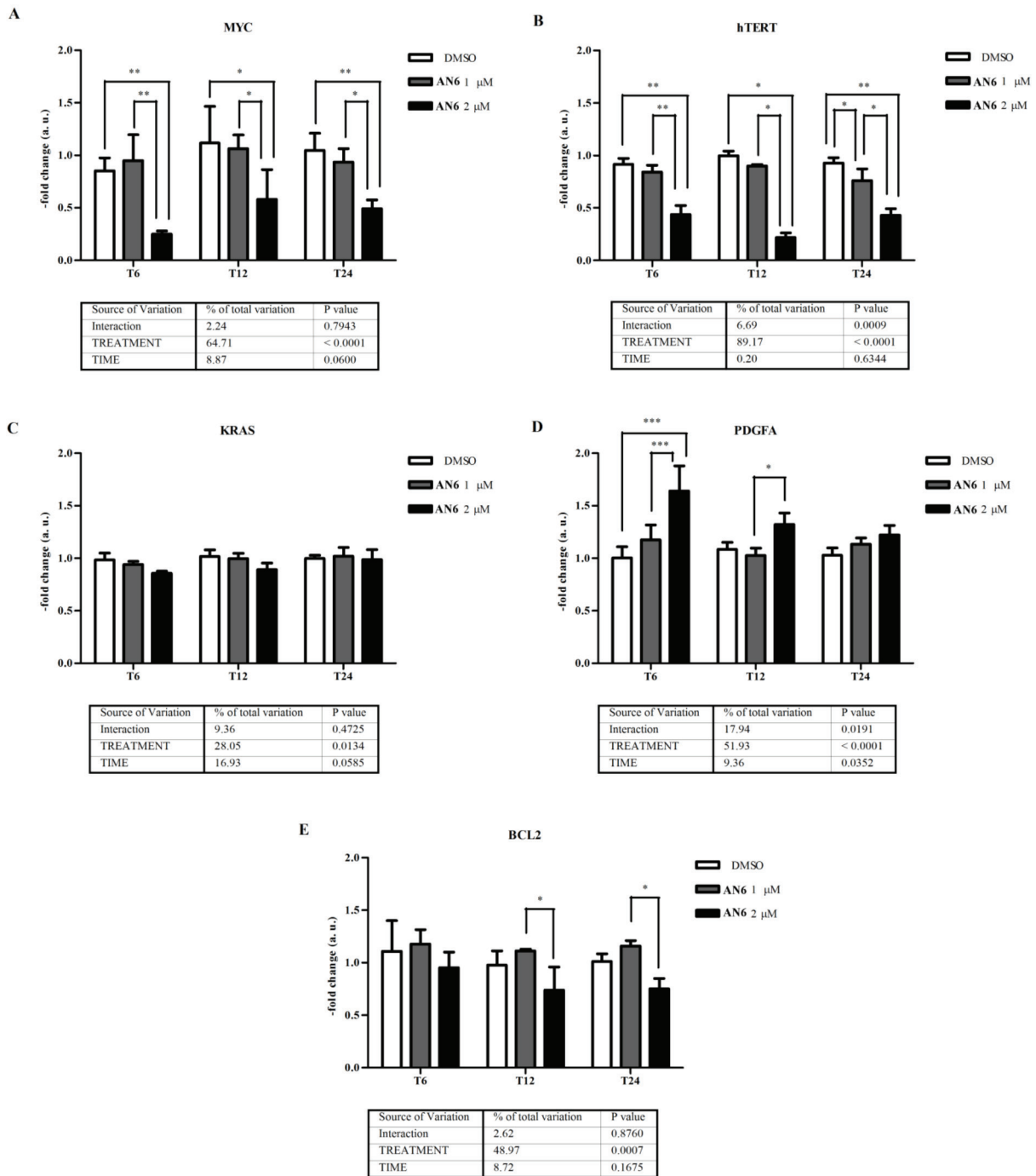


**Supplementary Figure S4: Effect of AN6 on *c-KIT* mRNA and protein expression in HGC27 and MCF7 cell lines.** *c-KIT* mRNA levels **A.** and **B.** were measured using a qPCR approach, and data (arithmetic means  $\pm$  S.D.) are expressed as n-fold change (a. u.) normalized to the RQ value of control cells at each time ( $T_6$ ,  $T_{12}$ ,  $T_{24}$ ), to whom an arbitrary value of 1 was assigned. The two-way ANOVA followed by Bonferroni post-test were used to identify statistical differences between ligand concentrations and time of treatment. The *c-kit* protein amount **C.** and **D.** was measured by flow cytometry, and data are expressed as n-fold change (%) of the mean fluorescence intensity (MFI) of untreated cells. The Student t-test was used to identify statistical differences between cells exposed to AN6 and those incubated with the vehicle (DMSO).\*:  $P < 0.05$ ; \*\*:  $P < 0.01$ .

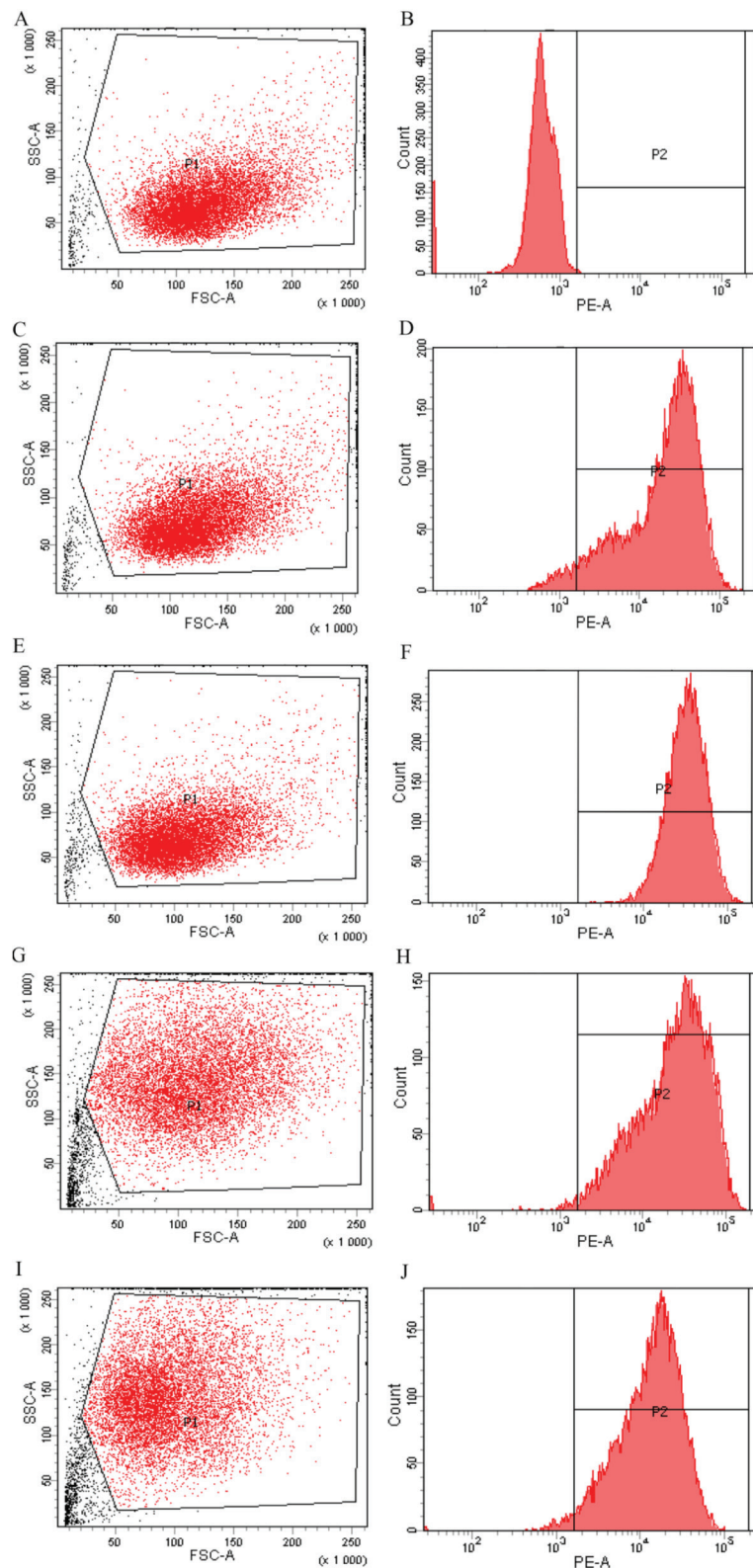


**Supplementary Figure S5: Effect of treatment with AN6 on mRNA of oncogenes possessing G4 structures in the HGC27 cell line.** A. *MYC*, B. *hTERT*, C. *KRAS*, D. *PDGFA*, E. *PDGFR $\beta$* , and F. *BCL2* mRNA levels were measured using qPCR assays, and data (arithmetic means  $\pm$  S.D.) are expressed as n-fold change (a.u.) normalized to the RQ of control cells at each time ( $T_6$ ,  $T_{12}$ ,  $T_{24}$ ) to which an arbitrary value of 1 was assigned. Two-way ANOVA and Bonferroni post-test were used to assess statistical differences between doses and time of treatment. \*, \*\*, \*\*\*:  $p < 0.05$ ;  $p < 0.01$ ;  $p < 0.001$ .

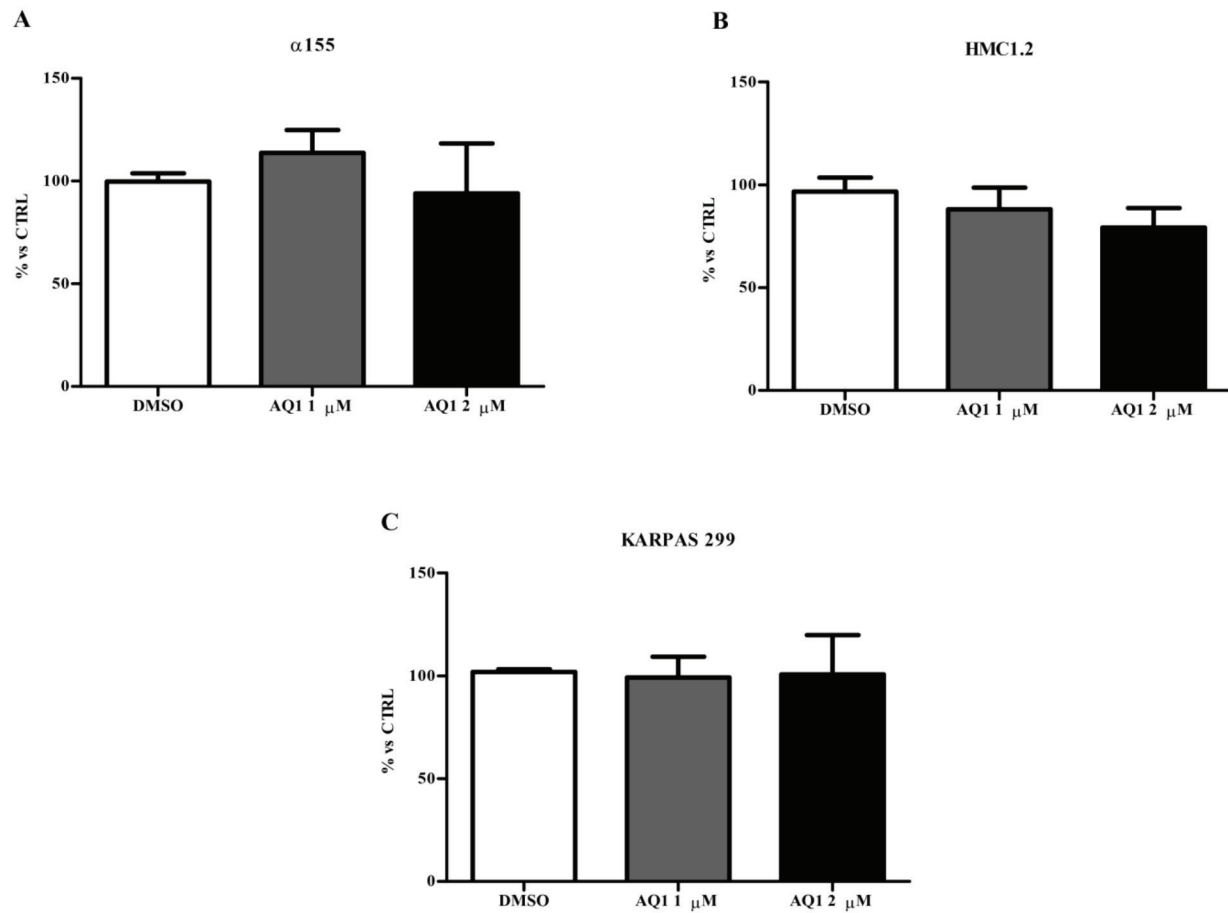




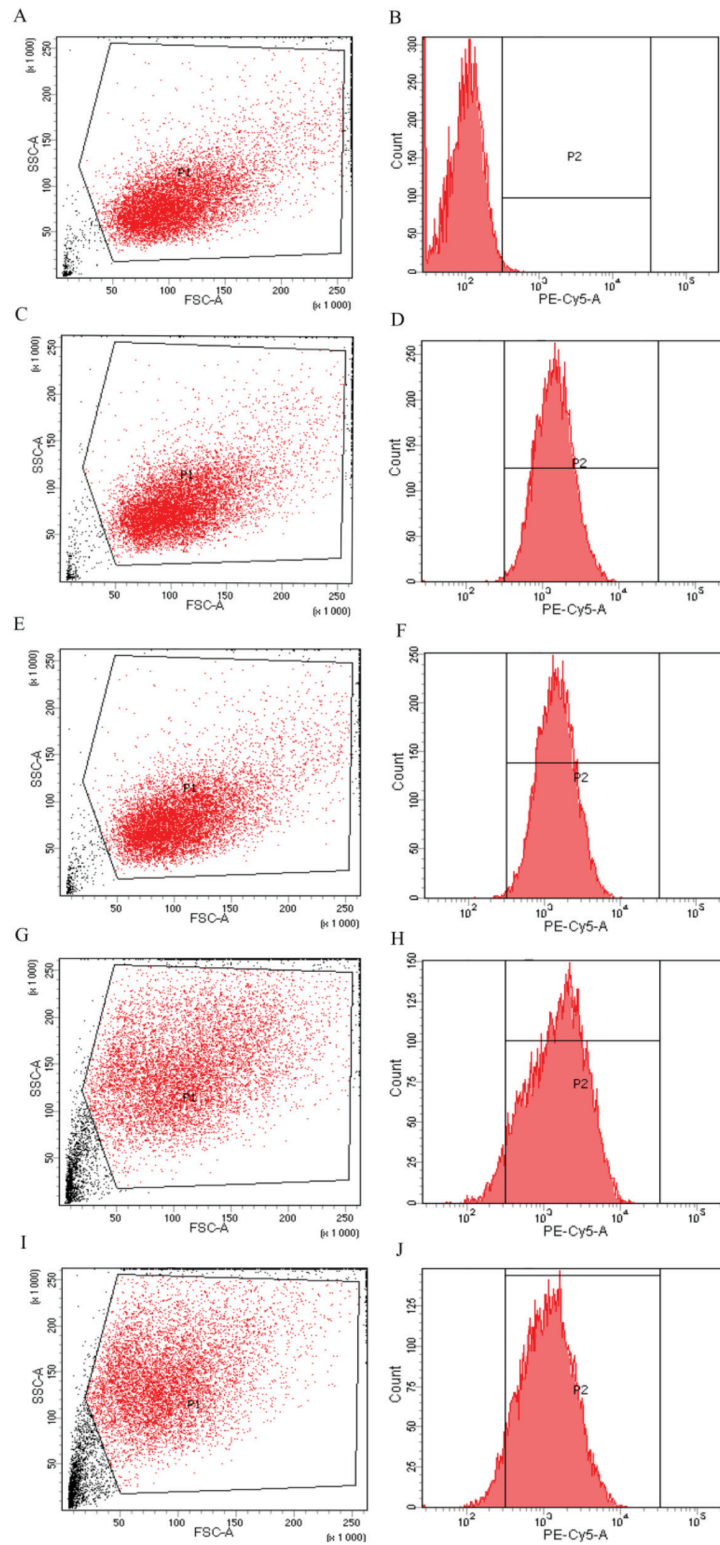
**Supplementary Figure S6: Effect of exposure with AN6 on mRNA of oncogenes possessing G4 structures in the MCF7 cell line.** A. *MYC*, B. *hTERT*, C. *KRAS*, D. *PDGFA* and E. *BCL2* mRNA level were measured by using a qPCR assay, and data (arithmetic means  $\pm$  S.D.) are expressed as n-fold change (a. u.) normalized to the RQ of control cells at each time (T<sub>6</sub>, T<sub>12</sub>, T<sub>24</sub>) to which an arbitrary value of 1 was assigned. Two-way ANOVA followed by Bonferroni post-test was used to assess statistical differences between doses and time of treatment. \*, \*\*, \*\*\*: p<0.05; p<0.01; p<0.001.



**Supplementary Figure S7: Flow cytometry analysis of CD117 in the  $\alpha 155$  cell line.** Morphological scatter plot with forward scatter (FSC) vs side scatter (SSC) and c-kit histogram plot of fluorescence intensity (FI) of different samples: **A.** and **B.** irrelevant antibody IgG; **C.** and **D.** control cells; **E.** and **F.** DMSO treated cells FI; **G.** and **H.** AQ1 1  $\mu$ M treated cells; **I.** and **J.** AQ1 2  $\mu$ M treated cells.



**Supplementary Figure S8: Effect of treatment with AQ1 on HLA proteins of  $\alpha$ 155 A. HMC1.2 B. and KARPAS299 C.** The HLA protein amounts were measured by flow cytometry and data are expressed as percentage of the fluorescence intensity (FI) measured in untreated cells (control). One-way ANOVA with Bonferroni post-test were used to assess statistical differences between cell treated with AQ1 and those treated with the vehicle (DMSO).



**Supplementary Figure S9: Flow cytometry analysis of HLA in  $\alpha 155$  cell line.** Morphological scatter plot with forward scatter (FSC) vs side scatter (SSC) and HLA histogram plot of fluorescence intensity (FI) of different samples. **A.** and **B.** irrelevant antibody IgG; **C.** and **D.** control cells; **E.** and **F.** DMSO treated cells FI; **G.** and **H.** AQ1 1  $\mu$ M treated cells; **I.** and **J.** AQ1 2  $\mu$ M treated cells.

**Supplementary Table S1: Library of tested compounds and variation of the melting temperature they induced at 1  $\mu$ M concentration of each tested DNA sequence**

Compounds	Ref.	Kit1	Kit2	HTS	dsDNA
HAD1	DB832 <sup>a</sup>	12.5	13.3	10.9	2.4
HAD2	DB1450 <sup>a</sup>	21.8	11.3	12.8	12.1
HAD3	DB2037 <sup>a</sup>	19.6	17.5	16.8	7.8
HAD4	DB1463 <sup>a</sup>	10.1	1.2	7.3	2.0
HAD5	DB1438 <sup>a</sup>	3.5	11.0	13.3	1.2
HAD6	DB1972 <sup>a</sup>	14.0	13.1	9.9	4.2
HAD7	DB1949 <sup>a</sup>	15.7	13.4	12.6	2.6
HAD8	DB934 <sup>a</sup>	7.4	5.8	5.0	2.9
HAD9	DB1693 <sup>a</sup>	12.1	9.5	9.4	2.2
HAD10	DB1694 <sup>a</sup>	10.6	13.9	5.6	1.1
HAD11	DB1093 <sup>a</sup>	12.9	13.4	11.7	11.5
HAD12	DB1999 <sup>a</sup>	8.1	13.1	4.9	2.4
NDI1	2 <sup>b</sup>	1.5	8.3	10.3	3.0
NDI2	1 <sup>b</sup>	0.6	0.7	9.2	2.8
NDI3	20 <sup>b</sup>	2.0	3.3	13.5	4.4
NDI4	22 <sup>b</sup>	0.4	0.7	7.0	1.9
NDI5	8 <sup>b</sup>	0.2	0.5	10.1	5.0
Phen1	K34 <sup>c</sup>	0.0	0.0	0.1	0.0
Phen1_Ni(II)	(K34) <sub>2</sub> Ni(II) <sup>c</sup>	1.9	0.0	3.1	0.0
Phen2	P120 <sup>d</sup>	0.0	0.0	0.1	0.0
Phen2_Ni(II)	(P120) <sub>2</sub> Ni(II) <sup>d</sup>	1.8	0.0	10.0	0.0
Phen3	P115 <sup>e</sup>	2.5	5.2	0.1	0.0
Phen3_Ni(II)	(P115)Ni(II) <sup>e</sup>	30.9	30.6	23.6	0.3
AQ1	D-13 <sup>f</sup>	13.1	15.3	18.0	4.6
AQ2	E-13 <sup>f</sup>	6.7	8.4	18.9	4.5
AQ3	B-13 <sup>f</sup>	9.9	12.9	14.2	2.5
AQ4	C-13 <sup>f</sup>	5.2	5.1	9.9	1.4
AQ5	D-15 <sup>f</sup>	10.2	6.0	18.2	1.2
AQ6	E-15 <sup>f</sup>	13.0	1.7	4.5	0.1
AQ7	B-15 <sup>f</sup>	9.5	11.1	7.0	0.3
AQ8	C-15 <sup>f</sup>	4.0	6.4	4.3	0.1
AN1	Ant1 <sup>g</sup>	0.0	2.4	1.0	1.2
AN2	Ant2 <sup>g</sup>	0.0	0.1	0.3	0.6
AN3	Ant9 <sup>g</sup>	0.0	0.2	1.0	1.6
AN4	Ant9,10 <sup>g</sup>	5.0	6.5	1.7	0.9

(Continued)

Compounds	Ref.	Kit1	Kit2	HTS	dsDNA
AN5	Ant1,5 <sup>g</sup>	2.0	6.7	13.6	0.5
AN6	Ant1,8 <sup>g</sup>	5.2	8.0	3.0	0.8
AN7	Ant2,6 <sup>g</sup>	4.4	7.2	4.7	0.1
AN8	Ant2,7 <sup>g</sup>	1.2	3.6	2.0	0.1

Errors were  $\pm 0.4$  °C. The compound name previously used and the corresponding reference are reported in the ref column.

<sup>a</sup>: Nanjunda R, Musetti C, Kumar A, Ismail MA, Farahat AA, Wang S, Sissi C, Palumbo M, Boykin DW, Wilson WD.

Heterocyclic dications as a new class of telomeric G-quadruplex targeting agents. *Curr Pharm Des.* 2012; 18: 1934-1947.

<sup>b</sup>: Milelli A, Tumiatti V, Micco M, Rosini M, Zuccari G, Raffaghello L, Bianchi G, Pistoia V, Díaz JF, Pera B, Trigili C, Barasoain I, Musetti C, et al. Structure-activity relationships of novel substituted naphthalene diimides as anticancer agents. *Eur J Med Chem.* 2012; 57: 417-428.

<sup>c</sup>: Musetti C, Lucatello L, Bianco S, Krapcho AP, Cadamuro SA, Palumbo M, Sissi C. Metal ion-mediated assembly of effective phenanthroline-based G-quadruplex ligands. *Dalton Trans.* 2009; 21: 3657-3660.

<sup>d</sup>: Bianco S, Musetti C, Krapcho AP, Palumbo M, Sissi C. Ni<sup>2+</sup> and Cu<sup>2+</sup> complexes of a phenanthroline-based ligand bind to G-quadruplexes at non-overlapping sites. *Chem Commun (Camb).* 2013; 49: 8057-8059.

<sup>e</sup>: Bianco S, Musetti C, Waldeck A, Sparapani S, Seitz JD, Krapcho AP, Palumbo M, Sissi C. Bis-phenanthroline derivatives as suitable scaffolds for effective G-quadruplex recognition. *Dalton Trans.* 2010; 39: 5833-5841.

<sup>f</sup>: Zagotto G, Ricci A, Vasquez E, Sandoli A, Benedetti S, Palumbo M, Sissi C. Tuning G-quadruplex vs double-stranded DNA recognition in regioisomeric lysyl-peptidyl-anthraquinone conjugates. *Bioconjug Chem.* 2011; 22: 2126-2135.

<sup>g</sup>: Folini M, Pivetta C, Zagotto G, De Marco C, Palumbo M, Zaffaroni N, Sissi C. Remarkable interference with telomeric function by a G-quadruplex selective bisantrene regioisomer. *Biochem Pharmacol.* 2010; 70: 1781-1790.

**Supplementary Table S2: qPCR and flow cytometry experimental settings chosen for each cell line and ligand tested in the study**

Cell line	Ligand	IC <sub>50</sub> (μM)	Ligand concentrations for qPCR assay (μM)	Analyzed exposure times (qPCR)	Ligand concentrations for flow cytometry assay (μM)	Analyzed exposure times (flow cytometry)
HCG27	AQ1	1.65	0.5 – 1.0	T6, T12, T24	1.0 – 2.0 <sup>a</sup>	T48
	AQ7	> 10.0	10.0 <sup>b</sup>	T6, T12, T24	--	--
	AN6	2.04	0.5 – 1.0	T6, T12, T24	1.0	T48
MCF7	AQ1	3.0	1.0 – 2.0	T6, T12, T24	1.0 – 2.0 <sup>a</sup>	T48
	AQ7	> 10.0	10.0 <sup>b</sup>	T6, T12, T24	--	--
	AN6	2.70	1.0 – 2.0	T6, T12, T24	1.0	T48
α155	AQ1	--	1.0	T6, T12	1.0 – 2.0	T48
HMC1.2	AQ1	--	1.0	T6, T12	1.0 – 2.0	T48

<sup>a</sup> 2 μM concentration was used only in BCL2 detection experiment (Figure 8); <sup>b</sup> data not shown in the manuscript.

**Supplementary Table S3: Primers and probes used for the qPCR analysis either obtained from previous publications or specifically designed for this study**

Gene	UPL <sup>a</sup> probe	Primers (5'- 3')	Source
<i>MYC</i> <sup>b</sup>	#67	F <sup>l</sup> : TGGTGCTCCATGAGGAGACA R <sup>m</sup> : GTGGCACCTCTTGAGGACCA	Gunaratnam et al., 2009
<i>PDGFA</i> <sup>c</sup>	#77	F: ACACGAGCAGTGTCAAGTGC R: CCTGCAGTATTCCACCTTGG	Iqbal et al., 2012
<i>PDGFRB</i> <sup>d</sup>	#14	R: TGCTCATCTGTGAAGGCAAG F: TGGCATTGTAGA AACTGCTCG	Chanakira et al., 2012
<i>BCL2</i> <sup>e</sup>	#75	F: ATGTGTGTGGAGAGCGTCAA R: GCCGTACAGTTCCACAAAGG	Brassesso et al., 2010
<i>B2M</i> <sup>f</sup>	#42	F: AGGCTATCCAGCGTACTCCA R: TGTCGGATGGATGAAACCCA	designed <i>ex novo</i>
<i>GAPDH</i> <sup>g</sup>	#60	F: CTCTGCTCCTCTGTTCGAC R: ACGACCAAATCCGTTGACTC	designed <i>ex novo</i>
<i>HPRT1</i> <sup>h</sup>	#22	F: TGATAGATCCATTCCTATGACTGTAGA R: CAAGACATTCTTTCCAGTTAAAGTTG	designed <i>ex novo</i>
<i>KIT</i> <sup>i</sup>	#29	F: GGCACGGTTGAATGTAAGGC R: CAGGGTGTGGGGATGGATTT	designed <i>ex novo</i>
<i>KRAS</i> <sup>j</sup>	#62	F: GGAGCTGGTGGCGTAGGCAAG R: GCCCTCCCCAGTCCTCATGT	designed <i>ex novo</i>
<i>hTERT</i> <sup>k</sup>	#68	F: GGAGAACAAGCTGTTTGCGG R: AGCCATACTCAGGGACACCT	designed <i>ex novo</i>

<sup>a</sup>Universal Probe Library; <sup>b</sup>V-Myc Avian Myelocytomatosis Viral Oncogene Homolog; <sup>c</sup>Platelet-Derived Growth Factor Alpha Polypeptide; <sup>d</sup>beta-type platelet-derived growth factor receptor; <sup>e</sup>B-cell lymphoma 2; <sup>f</sup>β-2-Microglobulin; <sup>g</sup>Glyceraldehyde-3-Phosphate Dehydrogenase; <sup>h</sup>Hypoxanthine Phosphoribosyltransferase 1; <sup>i</sup>V-Kit Hardy-Zuckerman 4 Feline Sarcoma Viral Oncogene Homolog; <sup>j</sup>Kirsten rat sarcoma viral oncogene homolog; <sup>k</sup>Telomerase Reverse Transcriptase; <sup>l</sup>forward; <sup>m</sup>reverse.

Supplementary Table S4: qPCR assay standard curve parameters obtained in MCF7 and HGC27 cell lines

Gene	MCF7			HGC27		
	Slope	Efficiency (%)	Dynamic range (Ct)	Slope	Efficiency (%)	Dynamic range (Ct)
<i>B2M</i>	-3,192	105,7	18,78 - 32,06	-3,34	99,1	18,74 - 30,85
<i>BCL2</i>	-3,41	96,5	25,82 - 34,13	-3,27	102,2	24,90 - 33,43
<i>GAPDH</i>	-3,48	93,7	15,81 - 30,59	-3,28	102	16,20 - 30,64
<i>HPRT1</i>	-3,324	99,9	20,23 - 32,63	-3,3	101	20,96 - 33,18
<i>KIT</i>	-3,137	108,3	29,01 - 35,78	-3,531	92	29,58 - 39,58
<i>KRAS</i>	-3,34	99	21,50 - 32,28	3,352	98,8	21,30 - 32,41
<i>MYC</i>	-3,3	100,7	26,85 - 33,06	-3,502	93	22,47 - 30,89
<i>PDGFA</i>	-3,169	106,8	22,97 - 31,68	-3,18	106,3	23,87 - 33,02
<i>PDGFRB</i>		Not expressed		-3,36	98,4	24,84 - 32,28
<i>hTERT</i>	-3,11		33,24 - 38,82	-3,34	99,2	29,38 - 35,78

Supplementary Table S5: qPCR assay standard curve parameters obtained in  $\alpha$ 155 and HMC1.2 cell lines

Gene	$\alpha$ 155			HMC1.2		
	Slope	Efficiency (%)	Dynamic range (Ct)	Slope	Efficiency (%)	Dynamic range (Ct)
<i>B2M</i>	-3.33	99.6	17.18-31.68	-3.38	97.7	17.46-31.25
<i>GAPDH</i>	-3.37	98	16.43-30.91	-3.40	96.7	17.34-31.36
<i>HPRT1</i>	-3.39	97.1	21.75-35.65	-3.38	97.5	22.14-37.67
<i>KIT</i>	-3.32	99.7	18.00-32.32	-3.30	101	19.08-32.90